LETTER

doi:10.1038/nature17154

The conformational signature of β-arrestin2 predicts its trafficking and signalling functions

Mi-Hye Lee[1], Kathryn M. Appleton[1], Erik G. Strungs[1], Joshua Y. Kwon[1], Thomas A. Morinelli[1], Yuri K. Peterson[2], Stephane A. Laporte[3,4,5] & Louis M. Luttrell[1,6]

Arrestins are cytosolic proteins that regulate G-protein-coupled receptor (GPCR) desensitization, internalization, trafficking and signalling[1,2]. Arrestin recruitment uncouples GPCRs from heterotrimeric G proteins, and targets the proteins for internalization via clathrin-coated pits[3,4]. Arrestins also function as ligand-regulated scaffolds that recruit multiple non-G-protein effectors into GPCR-based 'signalsomes'[5,6]. Although the dominant function(s) of arrestins vary between receptors, the mechanism whereby different GPCRs specify these divergent functions is unclear. Using a panel of intramolecular fluorescein arsenical hairpin (FlAsH) bioluminescence resonance energy transfer (BRET) reporters[7] to monitor conformational changes in β-arrestin2, here we show that GPCRs impose distinctive arrestin 'conformational signatures' that reflect the stability of the receptor–arrestin complex and role of β-arrestin2 in activating or dampening downstream signalling events. The predictive value of these signatures extends to structurally distinct ligands activating the same GPCR, such that the innate properties of the ligand are reflected as changes in β-arrestin2 conformation. Our findings demonstrate that information about ligand–receptor conformation is encoded within the population average β-arrestin2 conformation, and provide insight into how different GPCRs can use a common effector for different purposes. This approach may have application in the characterization and development of functionally selective GPCR ligands[8,9] and in identifying factors that dictate arrestin conformation and function.

The two non-visual arrestins, β-arrestin1 and β-arrestin2 (also known as arrestin2 and arrestin3, respectively), bind to and regulate the majority of extraretinal GPCRs[1,2]. Both static crystallographic structures[10–14] and biophysical studies in live cells[15,16] indicate that arrestins undergo conformational rearrangement on GPCR binding. To investigate the effect of GPCR activation on the dynamics of β-arrestin2 conformation and function, we prepared a series of FlAsH BRET probes[7] by inserting the six-amino-acid motif, CCPGCC, into the β-arrestin2 sequence at sites not predicted to be involved in its interactions with receptors or major binding partners (Fig. 1a). Each probe (rLuc–β-arrestin2–FlAsH1–6) was designed to measure BRET between a *Renilla* luciferase (rLuc) fluorescence donor at the amino terminus, and a fluorescein arsenical acceptor located at one of six positions along the length of β-arrestin2. We hypothesized that observing changes in BRET efficiency from multiple vantage points would yield an β-arrestin2 conformational signature that would correlate with its molecular functions. We first tested whether insertion of the FlAsH motif compromised β-arrestin2 recruitment by measuring the agonist-induced increase in intermolecular BRET between a C-terminal yellow fluorescent protein (YFP)-tagged GPCR and the N-terminal rLuc moiety of each rLuc–β-arrestin2–FlAsH construct. As shown in Fig. 1b, five of the rLuc–β-arrestin2–FlAsH constructs (F1, F2, F4, F5 and F6) generated BRET signals comparable to unmodified rLuc–β-arrestin2. The sixth construct (F3), which was poorly recruited, was included in subsequent experiments as an internal negative control. We then tested whether GPCR activation would produce an intramolecular rLuc–β-arrestin2–FlAsH BRET signal upon recruitment to an untagged GPCR. Agonist stimulation elicited changes in the β-arrestin2–FlAsH BRET signal (Δnet BRET) that were maintained over at least 10 min (Extended Data Fig. 1a) and proportional to receptor occupancy at less than saturating ligand concentration (Extended Data Fig. 1b). Thus, measuring the Δnet BRET of each construct produced a β-arrestin2–FlAsH BRET signature that was characteristic of the receptor being investigated (Fig. 1c). For the vasopressin type 2 receptor (V_2R), ligand stimulation caused significant decreases in the signal from FlAsH sensors in the N-terminal (F1 and F2) and C-terminal (F4 and F5) globular domains, and a significant increase in signal from the sensor located at the C terminus (F6). Predictably, given its poor recruitment, the F3 construct did not significantly change with stimulation.

To determine whether β-arrestin2–FlAsH signatures were conserved between GPCRs, we selected a panel of six additional receptors with diverse G-protein coupling, arrestin binding, and arrestin-dependent signalling characteristics (Extended Data Table 1). Our test panel included two stable arrestin-binding class 'B'[17] GPCRs: the angiotensin AT_{1A} receptor ($AT_{1A}R$) and the type 1 parathyroid hormone receptor (PTH_1R); three transient arrestin-binding class 'A'[17] GPCRs: the α_{1B}-adrenergic receptor ($\alpha_{1B}AR$), the β_2-adrenergic receptor (β_2AR), and the sphingosine-1-phosphate 1 receptor ($S1P_1R$); and the α_{2A}-adrenergic receptor ($\alpha_{2A}AR$) that does not produce detectable β-arrestin2 translocation. The G-protein-mediated signalling of each receptor was characterized using a FLIPR^{TETRA} fluorescent imaging plate reader to measure ligand-dependent activation or inhibition of adenylyl cyclase and stimulation of transmembrane Ca^{2+} entry[18] (Extended Data Fig. 2). The pattern of arrestin recruitment was confirmed by confocal fluorescence microscopy using GFP-tagged β-arrestin2 (ref. 19) (Fig. 2a). The β-arrestin2–FlAsH BRET signature generated by each receptor is shown in Fig. 2b. As the Δnet BRET observed with each probe reflects the 'population average' conformation of the cellular pool of rLuc–β-arrestin2–FlAsH, signatures were generated under conditions of receptor excess and saturating ligand concentration to ensure that the largest possible fraction of the reporter pool was receptor-bound at steady state. Inspection of the rLuc–β-arrestin2–FlAsH BRET signatures revealed that the class B receptors $AT_{1A}R$, PTH_1R and V_2R (Fig. 1c), which form stable GPCR–arrestin complexes that transit to endosomes[17], produced significant negative Δnet BRET signals at the F4 position and positive Δnet BRET signals at the C terminus (Fig. 2b; black arrows). In contrast, the class A $\alpha_{1B}AR$, β_2AR and $S1P_1R$, which dissociate from arrestin soon after internalization[17], produced little to no signal in these positions. Only small N-terminal responses were observed with $\alpha_{2A}AR$, which interacts weakly with β-arrestin2 (ref. 20).

[1]Department of Medicine, Medical University of South Carolina, Charleston, South Carolina 29425, USA. [2]Department of Pharmaceutical & Biomedical Sciences, College of Pharmacy, Medical University of South Carolina, Charleston, South Carolina 29425, USA. [3]Department of Medicine, McGill University Health Center Research Institute, McGill University, Quebec H4A 3J1, Canada. [4]Pharmacology and Therapeutics, McGill University, Quebec H3G 1Y6, Canada. [5]Anatomy and Cell Biology, McGill University, Quebec H3A 0C7, Canada. [6]Research Service of the Ralph H. Johnson Veterans Affairs Medical Center, Charleston, South Carolina 29401, USA.

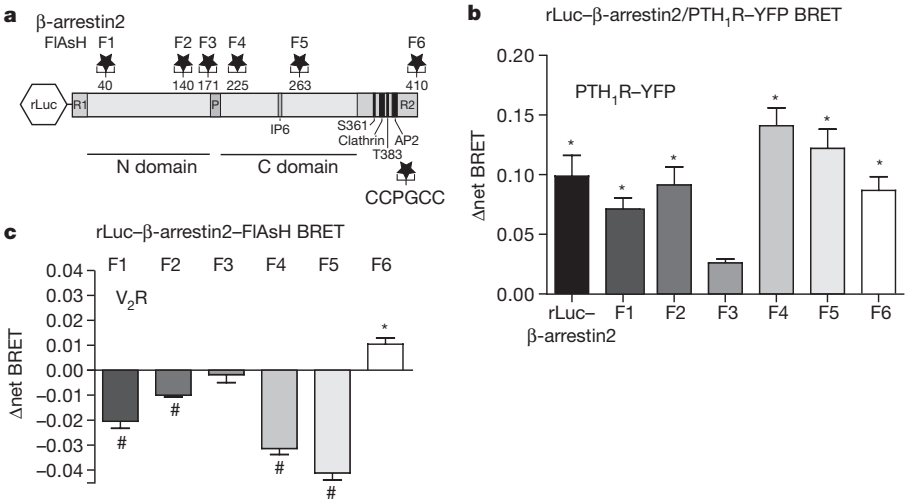

Figure 1 | Design and characterization of rLuc–β-arrestin2–FlAsH BRET reporters. a, Six rLuc–β-arrestin2–FlAsH BRET reporters (F1–F6) were constructed by inserting the amino acid motif CCPGCC after amino acid residues 40, 140, 171, 225, 263 and 410 of β-arrestin2. The location of each FlAsH motif is shown in relation to the globular N and C domains of β-arrestin2, as well as the clathrin and adaptor protein 2 (AP2) binding sites and reported phosphorylation sites (Ser^{361} and Thr^{383}) in the β-arrestin2 C-terminal regulatory (R2) domain[1]. **b**, Intermolecular BRET demonstrating ligand-dependent recruitment of rLuc–β-arrestin2–FlAsH1–6 to human PTH_1R. **c**, rLuc–β-arrestin2–FlAsH1–6 'signature' of β-arrestin2 binding to the V_2R. The bar graphs depict mean ± s.e.m. of independent biological replicates ($n = 3$ (**b**) and $n = 5$ (**c**)). $^*P < 0.05$, $^\#P < 0.005$, greater or less than vehicle-stimulated control.

To relate the β-arrestin2–FlAsH BRET signature to arrestin-dependent signalling, we determined the effect of silencing β-arrestin1/2 expression on ligand-stimulated ERK1/2 activation[21,22] using HEK293 FRT/TO β-arrestin1/2 shRNA cells that carry tetracycline-inducible shRNA targeting β-arrestin1/2 (ref. 23). As shown in Fig. 2c, ERK1/2 activation by $AT_{1A}R$, PTH_1R and $\alpha_{1B}AR$ was significantly attenuated by β-arrestin1/2 silencing, indicating a positive signalling role for arrestin scaffolds[24]. β-arrestin1/2 silencing had no net effect on ERK1/2 activation by β_2AR, which reportedly activates ERK1/2 via both $G_{i/o}$-dependent and arrestin-dependent pathways in HEK293 cells[25], and significantly enhanced ERK1/2 activation by the $S1P_1R$ and $\alpha_{2A}AR$, suggesting that for these receptors the major role of arrestins is to

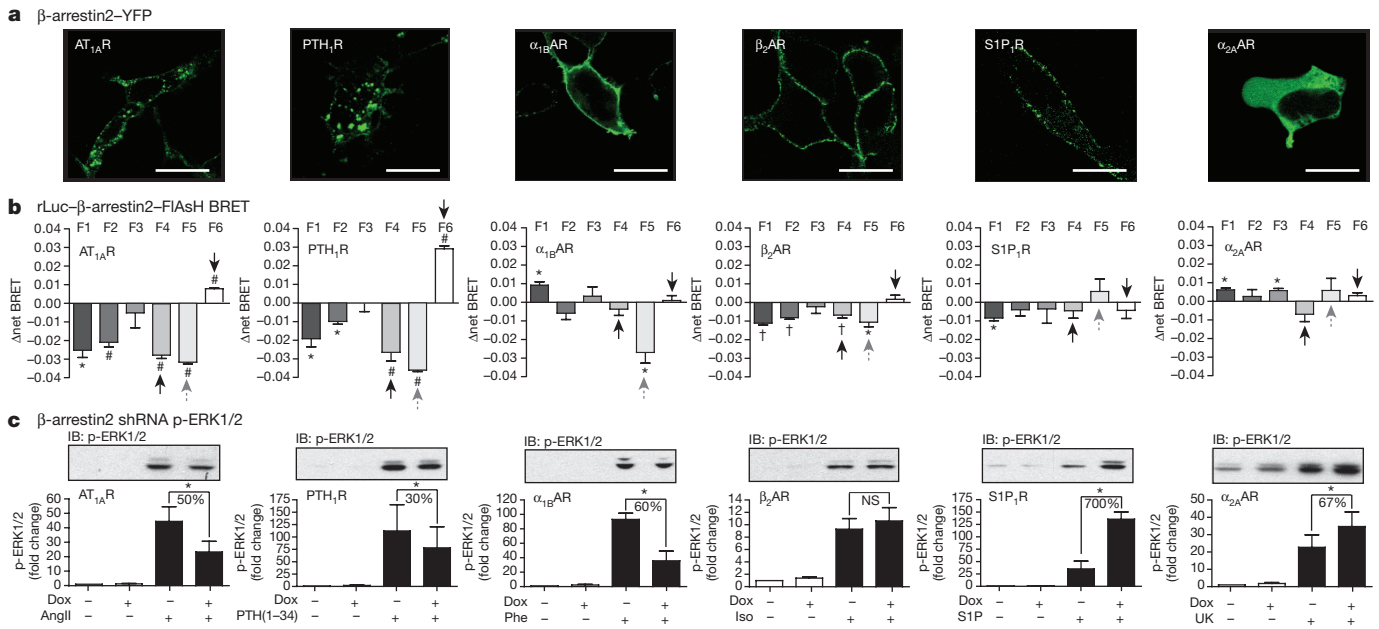

Figure 2 | Relationship between GPCR–β-arrestin2 complex formation, rLuc–β-arrestin2–FlAsH BRET signature, and arrestin-dependent ERK1/2 activation for six different GPCRs. a, Agonist-dependent recruitment of β-arrestin2–GFP. Each panel depicts a representative field of stimulated cells. β-arrestin2–GFP was diffusely cytosolic in the absence of agonist (not shown). Scale bars, 10 μm. **b**, Receptor-specific rLuc–β-arrestin2–FlAsH1–6 signatures. Each bar graph depicts mean ± s.e.m. of independent biological replicates ($n = 5$). $^*P < 0.05$, $^\#P < 0.005$, $^\dagger P < 0.001$, greater or less than vehicle-stimulated control. Black arrows indicate BRET changes related to GPCR–β-arrestin2 complex stability; grey arrows indicate changes related to β-arrestin2-dependent ERK1/2 activation. **c**, Effect of downregulating β-arrestin1/2 expression on GPCR-mediated ERK1/2 phosphorylation. A representative phospho-ERK1/2 immunoblot (IB) is shown above a bar graph depicting the mean ± s.e.m. of independent biological replicates ($n = 7$, $AT_{1A}R$; $n = 9$, PTH_1R; $n = 6$, $\alpha_{1B}AR$; $n = 20$, β_2AR; $n = 5$, $\alpha_{2A}AR$ and $S1P_1R$). Responses were normalized to the basal level of phospho-ERK1/2 in non-stimulated samples. Dox, doxycycline; iso, isoproterenol; phe, phenylephrine; PTH, parathyroid hormone N-terminal 1–34 fragment; S1P, sphingosine-1-phosphate; UK, UK14303. $^*P < 0.05$, greater or less than stimulated response in non-induced cells. NS, not significant.

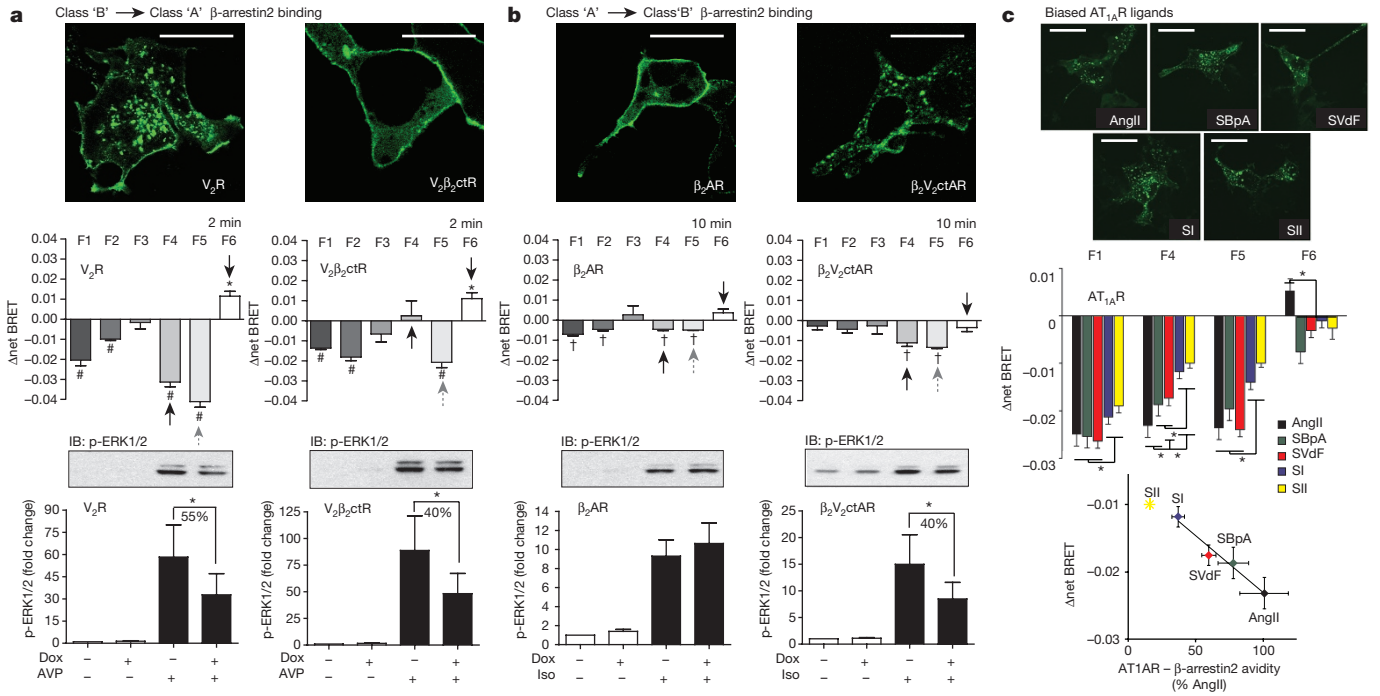

Figure 3 | Effect of GPCR–arrestin trafficking pattern and ligand structure on the rLuc–β-arrestin2–FlAsH BRET conformational signature. a, Effect of converting stable class B β-arrestin2 binding to transient class A binding. Upper, representative confocal fluorescence images showing the pattern of ligand-stimulated GFP–β-arrestin2 recruitment to the V_2R or the chimaeric $V_2\beta_2$ctR. Centre, the β-arrestin2–FlAsH1–6 profiles generated by V_2R and $V_2\beta_2$ctR. Lower, the arrestin-dependence of ERK1/2 phosphorylation by the V_2R and $V_2\beta_2$ctR. **b**, Analogous experiment demonstrating the effect of converting transient class A β-arrestin2 binding to stable class B binding using the β_2AR and the chimaeric $\beta_2V_2$ctAR. In **a** and **b**, phospho-ERK1/2 bar graphs depict mean ± s.e.m. of independent biological replicates ($n = 12$, V_2R and $V_2\beta_2$ctR; $n = 20$, β_2AR; $n = 12$ $\beta_2V_2$ctR). *$P < 0.05$, less than stimulated response in non-induced cells. Black arrows indicate BRET changes related to GPCR–β-arrestin2 complex stability; grey arrows indicate changes related to β-arrestin2-dependent ERK1/2 activation. **c**, Effect of ligand structure on the rLuc–β-arrestin2–FlAsH BRET signature. Upper, representative confocal fluorescence images showing the pattern of GFP–β-arrestin2 recruitment to the $AT_{1A}R$ upon stimulation with AngII, SBpA, SVdF, SI or SII. Centre, the F1 and F4–6 profiles generated by each ligand. Bottom, the relationship between the amplitude of the F4 signal and the independently determined avidity of $AT_{1A}R$ and β-arrestin2 measured by FRAP[27]. SII was not included in the linear fit, as the $AT_{1A}R$–β-arrestin2 avidity is too low to measure by FRAP. In all panels, the rLuc–β-arrestin2–FlAsH BRET graphs represent mean ± s.e.m. of independent biological replicates ($n = 5$, V_2R and $V_2\beta_2$ctR; $n = 6$, β_2AR and $\beta_2V_2$ctR; $n = 6$, $AT_{1A}R$, with each ligand). *$P < 0.05$, #$P < 0.005$, †$P < 0.001$, greater or less than vehicle-stimulated control. Scale bars, 10 μm.

dampen G-protein-dependent ERK1/2 activation by promoting desensitization. Consistent with this, we found that ERK1/2 activation via β_2AR, $S1P_1R$ and $\alpha_{2A}AR$ was strongly pertussis toxin-sensitive, indicating a predominantly $G_{i/o}$-mediated mechanism of activation (Extended Data Fig. 3). Comparison with the rLuc–β-arrestin2–FlAsH BRET signatures revealed a correlation between arrestin-dependent ERK1/2 activation and a significant negative Δnet BRET signal at the F5 position. This was most apparent for the class A $\alpha_{1B}AR$, which lacked the F4 and F6 signals characteristic of class B receptors, but retained the F5 signal shared by GPCRs mediating arrestin-dependent signals (Fig. 2b; grey arrows). The relationship between $\alpha_{1B}AR$-induced F5 signal and ERK1/2 activation was present over a range of agonist concentrations (Extended Data Fig. 4a), whereas at saturating ligand concentration the F5 signal readily separated the positive and negative roles of arrestin in ERK1/2 activation by our panel of seven GPCRs (Extended Data Fig. 4b).

We next examined chimaeric GPCRs in which the receptor C-tail was exchanged to reverse the class A and class B patterns of arrestin binding. As shown in Fig. 3a, replacing the C-tail of the class B V_2R with that of the class A β_2AR ($V_2\beta_2$ctR) is sufficient to reverse the arrestin binding pattern[26]. Although the C-tail exchange affected the stability of the receptor–arrestin complex, it did not affect arrestin-dependent ERK1/2 activation, which persisted in the $V_2\beta_2$ctR. Comparison of the rLuc–β-arrestin2–FlAsH BRET profiles generated by V_2R and $V_2\beta_2$ctR revealed that conversion of class B to class A binding caused the loss of the negative F4 signal characteristic of class B receptors such as $AT_{1A}R$, PTH_1R, and V_2R (Fig. 2b). In contrast, the F5 signal was preserved, such that the rLuc–β-arrestin2–FlAsH BRET signature of the chimaeric $V_2\beta_2$ctR resembled that of the $\alpha_{1B}AR$, the other class A GPCR that retained arrestin signalling. The opposite experiment, involving conversion of a class A receptor to class B, is shown in Fig. 3b. Replacing the C-tail of the class A β_2AR with that of the class B V_2R ($\beta_2V_2$ctR) reverses the arrestin binding pattern. In this case, $\beta_2V_2$ctR-mediated ERK1/2 activation became more arrestin-dependent, as evidenced by acquired sensitivity to shRNA silencing of β-arrestin1/2 expression. Inspection of the β-arrestin2–FlAsH BRET profiles of β_2R and $V_2\beta_2$ctR revealed that conversion of class A to class B produced a significant increase in the F4 signal that was most apparent following 10 min of ligand stimulation. Notably, the F5 signal also increased, consistent with the gain of arrestin-dependent signalling. Thus, reversing the stability of the arrestin–GPCR complex, without altering the other intracellular loops of the receptor, was sufficient to produce loss/gain of FlAsH BRET signal at the F4 position, whereas the magnitude of change in the F5 position correlated with arrestin-dependent signalling.

We then compared the β-arrestin2–FlAsH BRET signature generated by angiotensin II (AngII) with those of a previously characterized series of arrestin-selective 'biased' AngII analogues[27] (Fig. 3c). Although all five ligands—AngII, [Sar^1,Ile^4,Ile^8]-AngII (SII), [Sar^1,Ile^8]-AngII (SI), [Sar^1,Val^5,D-Phe^8]-AngII (SVdF) and [Sar^1,Val^5,Bpa^8]-AngII (SBpA)—promote the assembly of endosomal $AT_{1A}R$–arrestin complexes, fluorescence recovery after photobleaching (FRAP) has demonstrated that they cause different avidity between the receptor and β-arrestin2, with the rank order of receptor–arrestin complex half-life of AngII > SBpA > SVdF > SI > SII (ref. 27). The efficiency with which these

ligands promote arrestin-dependent ERK1/2 activation corresponds to the avidity of the complex, with longer half-life complexes generating proportionally greater arrestin-dependent signalling[27]. Inspection of the β-arrestin2–FlAsH BRET signatures demonstrated that although different ligands had little effect on the magnitude of the N-terminal F1 shift, the amplitude of the F4 and F5 signals were very sensitive to ligand structure. Plotting the F4 signal versus receptor–arrestin avidity measured by FRAP revealed a strong linear correlation. Thus, the signature presented by β-arrestin2–FlAsH BRET probes in the C-terminal domain reflected the avidity of the $AT_{1A}R$–β-arrestin2 interaction, even when comparing ligands that all evoke a canonical class B pattern of arrestin recruitment.

The rLuc–β-arrestin2–FlAsH BRET signature reflects both changes in the distance/orientation of the fluorophores due to conformational rearrangement, and steric effects generated by arrestin interaction with its receptor and non-receptor binding partners. Although it is not possible to ascribe the rLuc–β-arrestin2–FlAsH BRET signal at a given position to specific conformational shifts or engagement of binding partners, our data clearly demonstrate that ligand–GPCR complexes confer distinctive β-arrestin2 conformations, and that features of the conformational signature are conserved between receptors with similar arrestin binding/signalling characteristics. Moreover, we find that the Δnet BRET at selected positions correlates with downstream arrestin function, for example, class A versus class B trafficking and arrestin-dependent ERK1/2 activation, suggesting that β-arrestin2–FlAsH BRET probes can predict arrestin function on the basis of the ligand-induced conformational signature. Thus, intramolecular rLuc–β-arrestin2–FlAsH BRET probes may aid in identifying the factors that determine arrestin conformation and function, such as ligand 'bias'[8,9], GPCR C-tail 'phosphorylation codes' written by different GRKs[28], and post-translational modifications of arrestin that stabilize or destabilize the complex[29].

While this work was in progress, we became aware of a complementary study using β-arrestin2–FlAsH fluorescence resonance energy transfer (FRET) sensors[30]. This study confirms the existence of GPCR-specific β-arrestin2 conformations and, with the superior temporal resolution of FRET, provides key insights into the kinetics of receptor binding and arrestin activation.

Online Content Methods, along with any additional Extended Data display items and Source Data, are available in the online version of the paper; references unique to these sections appear only in the online paper.

Received 30 July 2015; accepted 19 January 2016.
Published online 23 March 2016.

1. Ferguson, S. S. Evolving concepts in G protein-coupled receptor endocytosis: the role in receptor desensitization and signaling. *Pharmacol. Rev.* **53,** 1–24 (2001).
2. Gurevich, V. V. & Gurevich, E. V. Structural determinants of arrestin functions. Prog. *Mol. Biol. Transl. Sci.* **118,** 57–92 (2013).
3. Goodman, O. B., Jr *et al.* β-Arrestin acts as a clathrin adaptor in endocytosis of the β_2-adrenergic receptor. *Nature* **383,** 447–450 (1996).
4. Laporte, S. A. *et al.* The β_2-adrenergic receptor/βarrestin complex recruits the clathrin adaptor AP-2 during endocytosis. *Proc. Natl Acad. Sci. USA* **96,** 3712–3717 (1999).
5. Shenoy, S. K. & Lefkowitz, R. J. Angiotensin II-stimulated signaling through G proteins and β-arrestin. *Sci. STKE* **2005**, cm14 (2005).
6. Luttrell, L. M. & Gesty-Palmer, D. Beyond desensitization: physiological relevance of arrestin-dependent signaling. *Pharmacol. Rev.* **62,** 305–330 (2010).
7. Hoffmann, C. *et al.* A FlAsH-based FRET approach to determine G protein-coupled receptor activation in living cells. *Nature Methods* **2,** 171–176 (2005).
8. Kenakin, T. Functional selectivity through protean and biased agonism: who steers the ship? *Mol. Pharmacol.* **72,** 1393–1401 (2007).
9. Luttrell, L. M. Minireview: More than just a hammer: ligand "bias" and pharmaceutical discovery. *Mol. Endocrinol.* **28,** 281–294 (2014).
10. Han, M. *et al.* Crystal structure of β-arrestin at 1.9 Å: possible mechanism of receptor binding and membrane translocation. *Structure* **9,** 869–880 (2001).
11. Zhan, X. *et al.* Crystal structure of arrestin3 reveals the basis of the difference in receptor binding between two non-visual subtypes. *J. Mol. Biol.* **406,** 467–478 (2011).
12. Shukla, A. K. *et al.* Structure of active β-arrestin-1 bound to a G-protein-coupled receptor phosphopeptide. *Nature* **497,** 137–141 (2013).
13. Kim, Y. J. *et al.* Crystal structure of pre-activated arrestin p44. *Nature* **497,** 142–146 (2013).
14. Kang, Y. *et al.* Crystal structure of rhodopsin bound to arrestin by femtosecond X-ray laser. *Nature* **523,** 561–567 (2015).
15. Charest, P. G., Terrillon, S. & Bouvier, M. Monitoring agonist-promoted conformational changes of β-arrestin in living cells by intramolecular BRET. *EMBO Rep.* **6,** 334–340 (2005).
16. Shukla, A. K. *et al.* Distinct conformational changes in β-arrestin report biased agonism at seven-transmembrane receptors. *Proc. Natl Acad. Sci. USA* **105,** 9988–9993 (2008).
17. Oakley, R. H., Laporte, S. A., Holt, J. A., Caron, M. G. & Barak, L. S. Differential affinities of visual arrestin, βarrestin1, and βarrestin2 for G protein-coupled receptors delineate two major classes of receptors. *J. Biol. Chem.* **275,** 17201–17210 (2000).
18. Appleton, K. M. *et al.* Biasing the parathyroid hormone receptor: relating *in vitro* ligand efficacy to *in vivo* biological activity. *Methods Enzymol.* **522,** 229–262 (2013).
19. Barak, L. S., Ferguson, S. S., Zhang, J. & Caron, M. G. A β-arrestin/green fluorescent protein biosensor for detecting G protein-coupled receptor activation. *J. Biol. Chem.* **272,** 27497–27500 (1997).
20. Wu, G. Krupnick, J. G., Benovic, J. L. & Lanier, S. M. Interaction of arrestins with intracellular domains of muscarinic and α_2-adrenergic receptors. *J. Biol. Chem.* **272,** 17836–17842 (1997).
21. DeFea, K. A. *et al.* β-Arrestin-dependent endocytosis of proteinase-activated receptor 2 is required for intracellular targeting of activated ERK1/2. *J. Cell Biol.* **148,** 1267–1281 (2000).
22. Luttrell, L. M. *et al.* Activation and targeting of extracellular signal-regulated kinases by β-arrestin scaffolds. *Proc. Natl Acad. Sci. USA* **98,** 2449–2454 (2001).
23. Zimmerman, B., Simaan, M., Lee, M.-H., Luttrell, L. M. & Laporte, S. A. c-Src-mediated phosphorylation of AP-2 reveals a general mechanism for receptors internalizing through the clathrin pathway. *Cell. Signal.* **21,** 103–110 (2009).
24. Wei, H. *et al.* Independent β-arrestin 2 and G protein-mediated pathways for angiotensin II activation of extracellular signal-regulated kinases 1 and 2. *Proc. Natl Acad. Sci. USA* **100,** 10782–10787 (2003).
25. Shenoy, S. K. *et al.* β-Arrestin-dependent, G protein-independent ERK1/2 activation by the β_2 adrenergic receptor. *J. Biol. Chem.* **281,** 1261–1273 (2006).
26. Oakley, R. H., Laporte, S. A., Holt, J. A., Barak, L. S. & Caron, M. G. Association of β-arrestin with G protein-coupled receptors during clathrin-mediated endocytosis dictates the profile of receptor resensitization. *J. Biol. Chem.* **274,** 32248–32257 (1999).
27. Zimmerman, B. *et al.* Differential β-arrestin-dependent conformational signaling and cellular responses revealed by angiotensin analogs. *Sci. Signal.* **5**, ra33 (2012).
28. Tobin, A. B., Butcher, A. J. & Kong, K. C. Location, location, location...site-specific GPCR phosphorylation offers a mechanism for cell-type-specific signalling. *Trends Pharmacol. Sci.* **29,** 413–420 (2008).
29. Kommaddi, R. P. & Shenoy, S. K. Arrestins and protein ubiquitination. *Prog. Mol. Biol. Transl. Sci.* **118,** 175–204 (2013).
30. Nuber, S. *et al.* β-Arrestin biosensors reveal a rapid, receptor-dependent activation/deactivation cycle. *Nature* http://dx.doi.org/10.1038/nature17198 (this issue).

Acknowledgements This work was supported by National Institutes of Health grants DK055524 (L.M.L.) and GM095497 (L.M.L.), funds provided by Dialysis Clinics, Inc. (T.A.M), and the Research Service of the Charleston, SC Veterans Affairs Medical Center (L.M.L.). Supported by Canadian Institutes of Health Research operating grant MOP-74603 (S.A.L.). National Institutes of Health grant RR027777 (L.M.L.) supported the $FLIPR^{TETRA}$ facility. The contents of this article do not represent the views of the Department of Veterans Affairs or the United States Government.

Author Contributions M.-H.L., K.A.M., E.G.S., J.Y.K, and S.A.L. performed experimental measurements and data analysis. T.A.M., Y.K.P., and S.A.L. provided technical expertise. M.-H.L. and L.M.L. conceived the project. All authors contributed to preparation of the manuscript and approved the final version.

Author Information Reprints and permissions information is available at www.nature.com/reprints. The authors declare no competing financial interests. Readers are welcome to comment on the online version of the paper. Correspondence and requests for materials should be addressed to L.M.L. (luttrell@musc.edu).

METHODS

Materials. Cell culture medium and cell culture additives were from Life Technologies. FuGENE HD transfection reagent and Promega GloSensor cAMP reagent were from Fisher Scientific. FLIPR Calcium 5 Assay Kit was from Molecular Devices, Inc. Lipofectamine 2000 and TC-FlAsH II In-Cell Tetracysteine Tag Detection Kits were from Invitrogen. Human PTH(1–34) was obtained from Bachem, Inc. Angiotensin II, [Arg^8]-vasopressin, isoproternol, phenylephrine, and UK14303 were from Sigma-Aldrich. S1P was from Avanti Polar Lipids Inc. SII was from MP Biomedicals. SI, SVdF and SBpA were synthesized at the Institut de Pharmacologie de Sherbrooke, Sherbrooke University. Rabbit polyclonal anti-β-arrestin1/2was a gift from R.J. Lefkowitz. Anti-phospho-ERK1/2 IgG (T202/Y204; #9101) and anti-ERK1/2 IgG (#4695) were from Cell Signaling Technology. Horseradish-peroxidase-conjugated donkey anti-rabbit IgG was from Jackson Immuno-Research Laboratories, Inc.

***Renilla* luciferase–β-arrestin2 FlAsH BRET reporters.** The pcDNA3.1 plasmid encoding rat β-arrestin2 tagged at the N terminus with *Renilla* luciferase (rLuc) was a gift from M. Bouvier. A series of six rLuc–β-arrestin2–FlAsH BRET reporters were constructed by inserting a cDNA sequence encoding the amino acid motif, CCPGCC, immediately following amino acid residues 40, 140, 171, 225, 263 and 410 of β-arrestin2, using a modification of the precise gene fusion PCR method[31]. For each construct, two PCR steps were performed using the primer sets shown in Extended Data Table 2. The first step was to generate two PCR fragments using the primer pairs: RlucHindF–FlAsHR and FlAsAF–RlucApalR. One PCR product contained a HindIII restriction site at the 5′ end and the CCPGCC FlAsH motif at the 3′ end, and the other contained the complementary FlAsH sequence at the 5′ end and an ApaI restriction site at the 3′ end. A second PCR step was used to fuse the two fragments using three primers: RlucHindF, FlAsHR and RluApalR, and the two PCR fragments as template DNA. The resultant full-length β-arrestin2 PCR product containing the FlAsH motif insert was digested with HindIII and ApaI and cloned into the parent rLuc–β-arrestin2 plasmid to generate the rLuc–β-arrestin2–FlAsH1–6 expression plasmids. All constructs were verified by dideoxynucleotde sequencing.

Cell culture and transfection. HEK293 cells (ATCC CRL1573) were from the American Type Culture Collection. HEK-293 GloSensor cells were from Promega Corporation. HEK293 cells were maintained in minimum essential medium supplemented with 10% fetal bovine serum and 1% antibiotic/antimycotic solution. The HEK293 FRT/TO β-arrestin1/2 shRNA cell line carrying tetracycline-inducible shRNA simultaneously targeting the β-arrestin1 and 2 isoforms (5′-CGTCCACGTCACCAACAAC-3′) was generated as previously described[23]. These cells were maintained in Dulbecco's modified Eagle medium supplemented with 10% fetal bovine serum, 1% antibiotic/antimycotic solution and 50 μg ml^{-1} zeocin, 50 μg ml^{-1} blasticidin, and 50 μg ml^{-1} puromycin to maintain selection. Transient transfections were performed using Lipofectamine 2000 or FuGENE HD according to the manufacturer's protocols. Before experimentation, cells were serum-deprived overnight in 1% fetal bovine serum growth medium. Cells were not tested for mycoplasma contamination.

FLIPR^{TETRA} assay of calcium influx. HEK293 cells in 6-well plates were transiently transfected with 1 μg of plasmid cDNA encoding the angiotensin AT$_{1A}$, PTH$_1$R, α_{1B}AR, β_2AR, S1P$_1$R or α_{2A}AR, using Lipofectamine 2000. Cells were seeded onto collagen-coated black-wall clear-bottom 96-well plates (BD Biosciences) 24 h after transfection, allowed to grow for a further 24 h, then serum deprived overnight. Fresh FLIPR calcium 5 assay reagent (100 μl per well) was added to 100 μl of serum-deprivation medium and plates were incubated for an additional 1 h before stimulation. Stimulations were carried out on a FLIPR^{TETRA} (Molecular Devices) with 470–495 nm excitation and 515–575 nm emission filters as previously described[18]. All assays were performed using saturating ligand concentrations: AngII (0.1 μM), hPTH(1–34) (0.1 μM), isoproterenol (1 μM), phenylephrine (10 μM), S1P (1 μM) or UK14303 (10 μM) and run at room temperature. The instrument was programmed to simultaneously dispense 50 μl of vehicle control, 5× ligand, or the calcium ionophore A23187 (10 μM) from the drug plate into the 200 μl of medium in the corresponding wells of the assay plate to achieve the final ligand concentration. Fluorescence was recorded every 1 s for 10 reads to establish baseline fluorescence, then every 1 s for 300 reads. Raw data representing the relationship between time and fluorescence for each well were exported to Microsoft Excel for background subtraction and analysis.

FLIPR^{TETRA} assay of cAMP production. Assays were performed using HEK293 GloSensor cAMP cells that stably express a genetically encoded biosensor composed of a cAMP binding domain fused to a mutated form of *Photinus pyralis* luciferase[32]. HEK293 GloSensor cAMP cells were seeded onto poly-D-lysine-coated white-wall clear-bottom 96-well plates (BD Biosciences) 24 h after transient transfection with plasmid cDNA encoding the receptors of interest. cAMP assays were performed 72 h after transfection as previously described[18]. cAMP reagent medium was prepared by adding 200 μl of freshly thawed GloSensor cAMP reagent to 10 ml of serum free MEM buffered with 10 mM HEPES (pH 7.4). The growth medium was gently aspirated and replaced with 100 μl per well of pre-warmed cAMP reagent medium. Plates were incubated at 37 °C with 5% CO_2 for 1.5 h, then removed from the incubator and incubated at room temperature in the dark for an additional 30 min. Stimulations were performed at room temperature in the FLIPR^{TETRA} using saturating ligand concentrations. Luminescence was recorded every 1 s for 10 reads to establish baseline luminescence, then every 1 s for 50 reads. Thereafter, luminescence was recorded every 2 s for 600 reads. Raw data representing the relationship between time and luminescence for each well following ligand addition was exported to Microsoft Excel for background subtraction and analysis. All responses were normalized to the cAMP luminescence generated in response to 10 μM forskolin. To assay G$_i$-mediated inhibition of cAMP production ($\alpha 2_{2A}$R and S1P$_1$R), cells were pre-incubated with or without agonist for 30 min, then stimulated with 10 μM forskolin.

Intermolecular BRET using rLuc–β-arrestin2 and PTH$_1$R–YFP. HEK 293 cells were transiently transfected with 1.5 μg of plasmid DNA encoding the C-terminal yellow fluorescent protein (YFP)-tagged PTH$_1$R[33] and 0.15 μg of either rLuc–β-arrestin2 or one of the rLuc–β-arrestin2–FlAsH constructs using Fugene HD. Cells were detached 48 h after transfection, collected by centrifugation, resuspended in BRET buffer (1 mM $CaCl_2$, 140 mM NaCl, 2.7 mM KCl, 900 μM $MgCl_2$, 370 μM NaH_2PO_4, 5.5 mM D-glucose, 12 mM $NaHCO_3$, 25 mM HEPES (pH 7.4)) and aliquotted into white-wall clear-bottom 96-well plates at a density of 100,000 cells per well. Background and total Venus fluorescence were read on an OptiPlate microplate reader (PerkinElmer) with 485 nm excitation and 525–585 nm emission filters. Cells were stimulated with 0.1 μM PTH(1–34) for 2 min and coelenterazine was then added to a final concentration of 5 μM. Luciferase (440–480 nm) and Venus (525–585 nm) emissions were read to calculate the BRET ratio (emission eYFP/emission Rluc). Net BRET ratio was calculated by background subtracting the BRET ratio measured for vehicle- versus ligand-treated cells in the same experiment.

Intramolecular FlAsH BRET using the rLuc–β-arrestin2–FlAsH constructs. HEK293 cells seeded in 6-well plates were co-transfected with 1.5 μg of plasmid DNA encoding the receptor of interest and 0.1 μg of DNA encoding one rLuc–β-arrestin2–FlAsH construct using Fugene HD. Cells were detached 48 h after transfection, collected by centrifugation, and resuspended in 600 μl of Hank's balanced salt solution. TC-FlAsH II In-Cell Tetracystein detection reagent was added at 2.5 μM final concentration and the cells incubated at room temperature for 30 min, after which they were washed using 1× BAL buffer from the TC-FlAsH kit, resuspended in BRET buffer and placed in white-wall clear-bottom 96-well plates at a density of 100,000 cells per well. Background and total TC-FlAsH fluorescence were read on an Optiplate microplate reader (Perkin-Elmer) with 485 nm excitation and 525–585 nm emission filters. Except as noted in the figure legends, all stimulations were carried out at saturating ligand concentration: AngII (0.1 μM), [Arg^8]–vasopressin (1 μM), hPTH(1–34) (0.1 μM), isoproterenol (1 μM), phenylephrine (10 μM), S1P (1 μM), SBpA (1 μM), SII (1 μM) SVdF (1 μM), or UK14303 (10 μM). Cells were exposed to agonist for 2–10 min, after which coelenterazine was added at a final concentration of 5 μM. Six consecutive readings of luciferase (440–480 nm) and TC-FlAsH (525–585 nm) emissions were taken, and the BRET ratio (emission eYFP/emission Rluc) calculated using Berthold Technologies Tristar 3 LB 941. The Δnet change in intramolecular BRET ratio for each of the six rLuc–β-arrestin2–FlAsH constructs was calculated by background subtracting the BRET ratio measured for cells in the same experiment stimulated with vehicle only.

Confocal microscopy. For determining the pattern of GPCR–arrestin trafficking, HEK293 cells were seeded into collagen-coated 35 mm glass-bottom Petri dishes (MatTek Corporation) and co-transfected with 1.3 μg of plasmid DNA encoding the receptors of interest and 0.7 μg of plasmid encoding green fluorescent protein (GFP)-tagged β-arrestin2[19] using FuGene HD. Forty-eight hours after transfection, cells were serum derived for 4 h, stimulated with a saturating ligand concentration for 8 min, fixed with 4% paraformaldehyde in phosphate buffered saline for 30 min and washed with 4 °C saline. Arrestin distribution was determined by confocal microscopy performed on a Zeiss LSM510 META laser-scanning microscope with 60× objective using 488 nm excitation and 505–530 nm emission wavelengths. Measurement of AT$_{1A}$R–β-arrestin2 avidity was performed as previously described[27]. HEK293 cells stably expressing AT$_{1A}$R and transfected with β-arrestin2–YFP were stimulated with AngII (1 μM) or analogues (10 μM) for 15 min, after which, endosomes were bleached and fluorescence recovery was monitored every 30 s over a period of 5 min.

Immunoblotting. HEK293 FRT/TO β-arrestin1/2 shRNA cells were used to determine the contribution of arrestins to GPCR-stimulated ERK1/2 activation[23,34]. Cells in 12-well plates were transiently transfected with 1 μg of plasmid cDNA encoding the receptor of interest using FuGENE HD. Twenty-four hours after transfection, downregulation of β-arrestin1/2 expression was induced by 48 h exposure to 1 μM doxycycline. After overnight serum deprivation, cells were stimulated

for 5 min, after which monolayers were lysed in 1× Laemmli sample buffer. Stimulations were performed at saturating ligand concentration, except as noted in the figure legends. Lysates containing 10 μg of whole-cell protein were resolved by sodium dodecyl sulphate polyacrylamide gel electrophoresis and transferred to polyvinylidine difluoride membranes. Immunoblots of phospho-ERK1/2, total ERK1/2, and β-arrestin1/2 were performed using rabbit polyclonal IgG with HRP-conjugated goat anti-rabbit IgG as secondary antibody. Proteins were visualized using enhanced chemiluminescence (PerkinElmer).

Statistical analysis. The sample size (n) reported in each figure legend refers to number of independently performed biological replicates in the data set. All analysable data points were included in the statistical analyses. No statistical methods were used to predetermine sample size. For experimental methods that were highly reproducible, for example, measurement of Δnet BRET, 5 to 6 biological replicates were sufficient to discern effects of ±0.01 with $P < 0.05$. For experimental methods with greater variability between replicates, for example, fold ERK1/2 activation, 5 to 20 biological replicates were necessary to discern effects of β-arrestin1/2 silencing that were ±10% of the control response with $P < 0.05$. The investigators were not blinded to allocation during experiments and outcome assessment. All values are expressed as mean ± s.e.m. ($n \geq 5$). For comparisons between two groups, statistical significance was assessed with a two-tailed unpaired t-test. Computations were performed and graphs constructed with the GraphPad Prism 4.0 scientific graphing, curve fitting, and statistics program (GraphPad Software). The experiments were not randomized.

31. Yon, J. & Fried, M. Precise gene fusion by PCR. *Nucleic Acids Res.* **17,** 4895 (1989).
32. Binkowski, B. F., Fan, F. & Wood, K. V. Luminescent biosensors for real-time monitoring of intracellular cAMP. *Methods Mol. Biol.* **756,** 263–271 (2011).
33. Leonard, A. P., Appleton, K. M., Luttrell, L. M. & Peterson, Y. K. A high-content, live-cell, and real-time approach to the quantitation of ligand-induced β-arrestin2 and class A/class B GPCR mobilization. *Microsc. Microanal.* **19,** 150–170 (2013).
34. Wilson, P. C. *et al.* The arrestin-selective angiotensin AT1 receptor agonist [Sar^1,Ile^4,Ile^8]-AngII negatively regulates bradykinin B2 receptor signaling via AT1-B2 receptor heterodimers. *J. Biol. Chem.* **288,** 18872–18884 (2013).

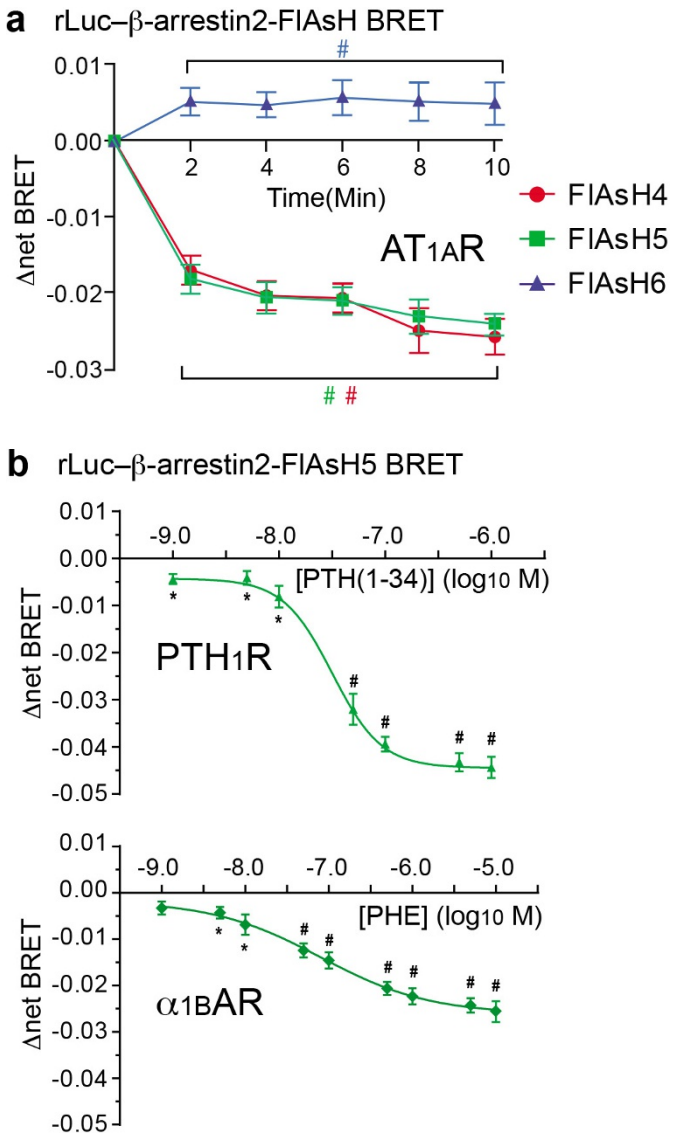

Extended Data Figure 1 | Time-course and relationship of the β-arrestin2 intramolecular FlAsH BRET signal to receptor occupancy. **a**, Time-course of $AT_{1A}R$-induced changes in intramolecular FlAsH BRET. HEK293 cells were co-transfected with plasmid cDNA encoding $AT_{1A}R$ and the indicated rLuc–β-arrestin2–FlAsH reporter. Stimulations were carried out at a saturating concentration of AngII for the indicated times. The graph depicts the mean ± s.e.m. of independent biological replicates of ligand-induced Δnet BRET for each rLuc–β-arrestin2–FlAsH construct ($n = 6$). **b**, Ligand concentration dependence of PTH_1R- and $\alpha_{1B}AR$-induced changes in intramolecular FlAsH BRET. HEK293 cells were co-transfected with plasmid cDNA encoding the PTH_1R or $\alpha_{1B}AR$ and the rLuc–β-arrestin2–FlAsH5 reporter. Stimulations were for 2 min using the indicated agonist concentration. The graph depicts the mean ± s.e.m. of independent biological replicates of ligand-induced Δnet BRET ($n = 5$). The EC_{50} for PTH(1–34) (PTH_1R) and phenylephrine ($\alpha_{1B}AR$) were 30 nM and 80 nM, respectively. In all panels: $^*P < 0.05$, $\#P < 0.005$, greater or less than vehicle stimulated control.

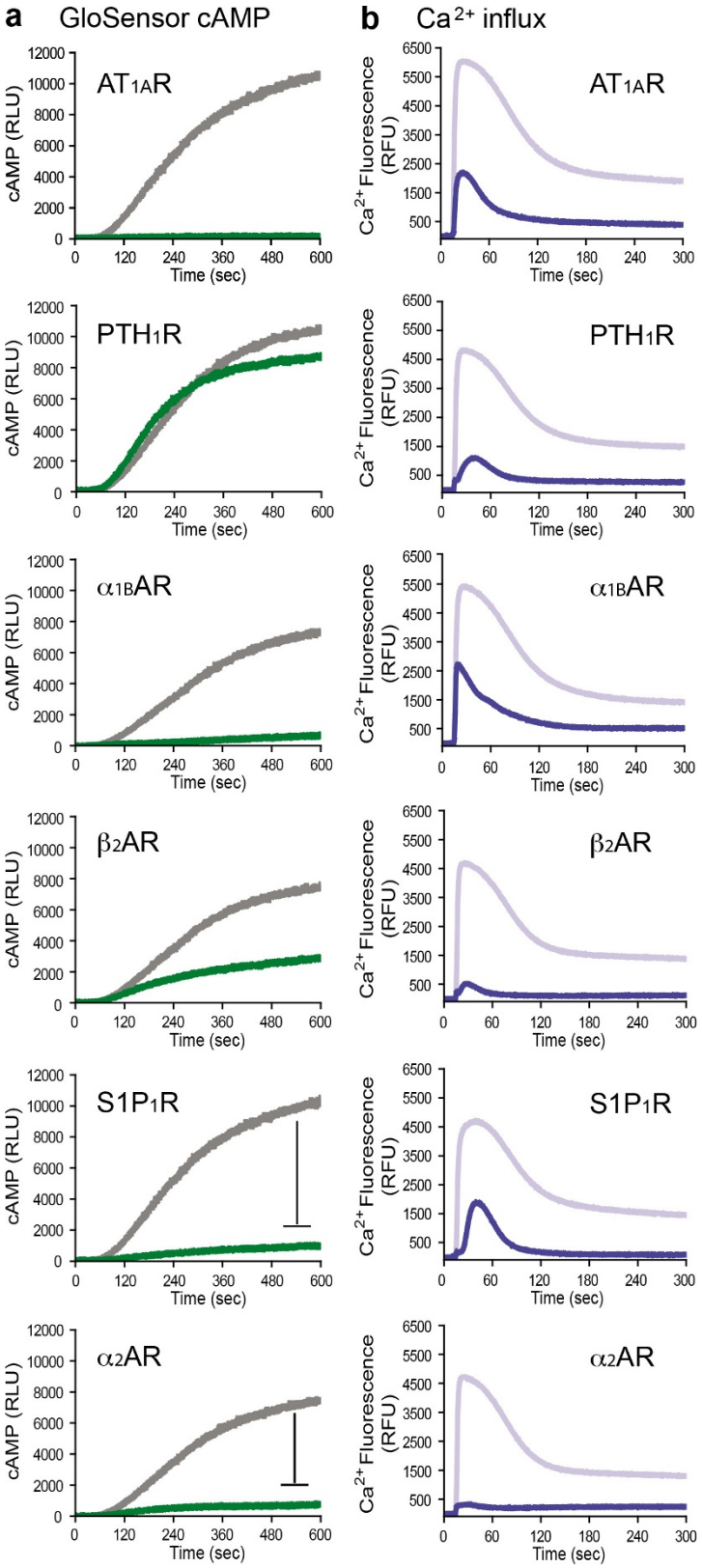

Extended Data Figure 2 | G-protein-coupling profiles of selected GPCRs. a, Representative time-courses of cAMP luminescence following stimulation of HEK293 GloSensor cAMP cells transfected with each of six GPCRs. For the $G_{i/o}$-coupled $S1P_1R$ and $\alpha_{2A}AR$, stimulations were carried out in the presence of 10 μM forskolin to detect inhibition of adenylyl cyclase. Each panel depicts the agonist effect (green) compared to the control response to 10 μM forskolin (grey) measured in adjacent wells. Data are presented in relative luminescence units (RLU). **b**, Representative time-courses of intracellular calcium fluorescence following stimulation of HEK293 cells transfected with the same panel of GPCRs. Each panel depicts the agonist effect (blue) compared to the control response to the calcium ionophore A23187 (lavender) measured in adjacent wells. Data are presented in relative fluorescence units (RFU).

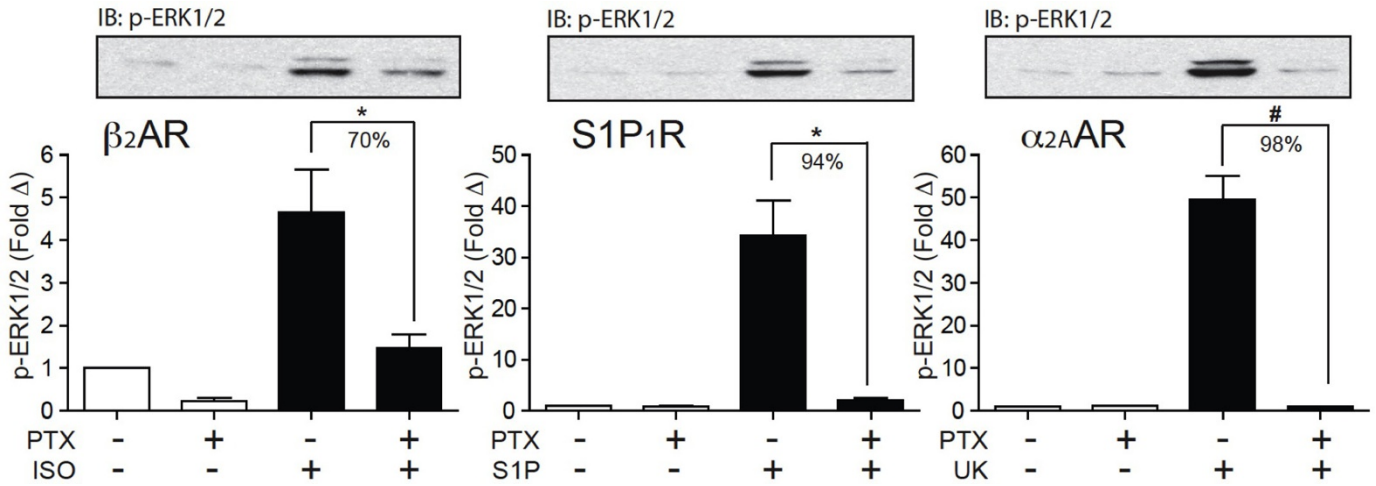

Extended Data Figure 3 | Pertussis toxin sensitivity of ERK1/2 activation by $G_{i/o}$-coupled GPCRs . HEK293 cells transfected with the β_2AR, S1PR$_1$ or α_{2A}AR were serum-deprived overnight in the presence or absence of 1 ng ml^{-1} *Bordetella pertussis* toxin (PTX) before 5 min stimulation with isoproterenol, S1P or UK14303, respectively. Representative phospho-ERK1/2 immunoblots are shown above bar graphs depicting the mean ± s.e.m. of independent biological replicates ($n = 5$, β_2AR, S1P$_1$R and α_{2A}AR). Responses were normalized to the basal level of phospho-ERK1/2 in non-stimulated samples. *$P < 0.05$, #$P < 0.005$, less than stimulated response in the absence of pertussis toxin.

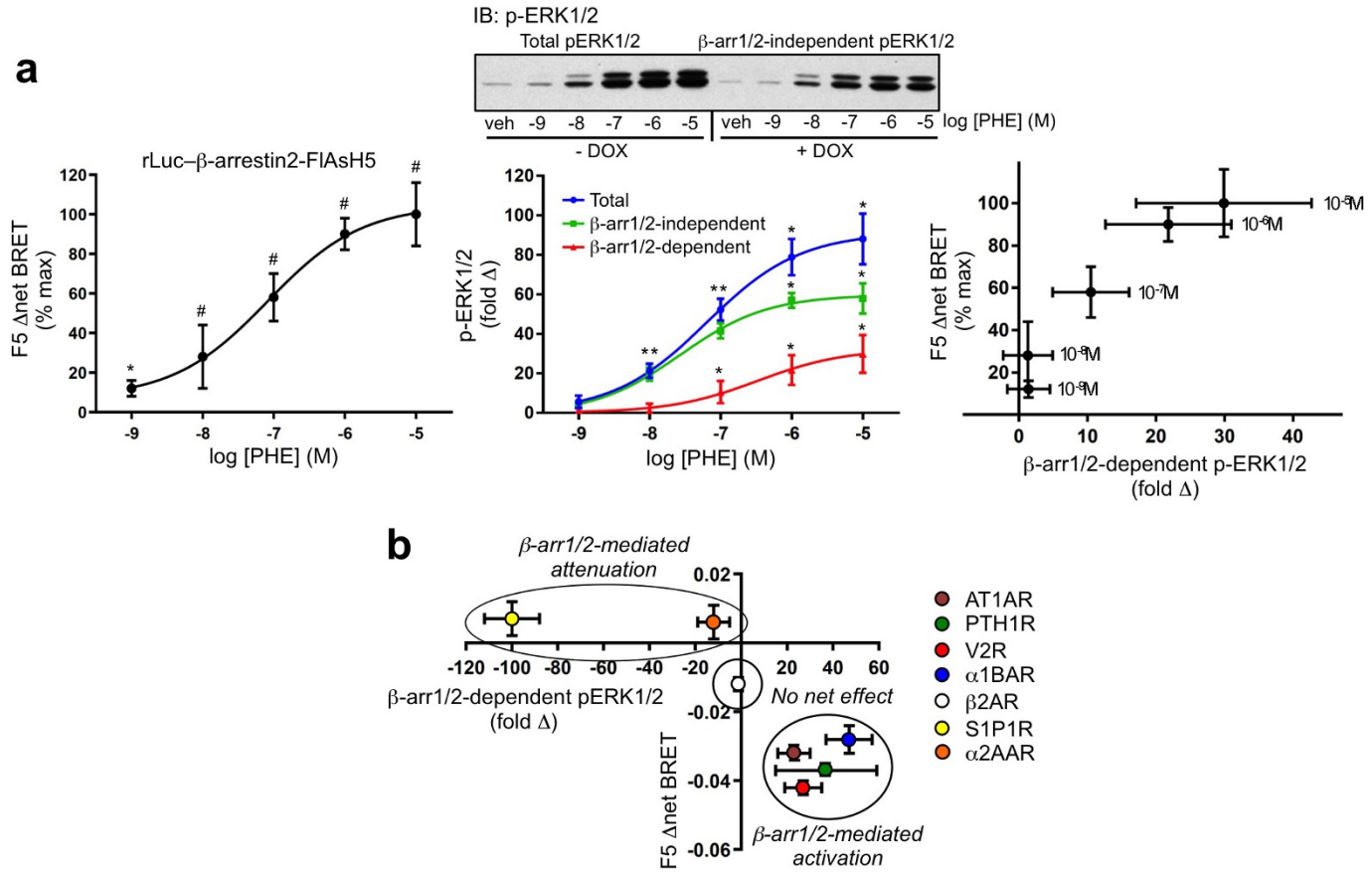

Extended Data Figure 4 | Concentration-response relationship between FlAsH5 signal and arrestin-dependent ERK1/2 activation. **a**, Relationship between α_{1B}AR-induced change in FlAsH5 Δnet BRET and arrestin-dependent ERK1/2 activation at varying agonist concentration. The percent maximal phenylephrine-induced FlAsH5 Δnet BRET was determined in HEK293 cells transfected with α_{1B}AR and rLuc–β-arrestin2–FlAsH5 expression plasmids (left). The concentration dependence of phenylephrine-stimulated ERK1/2 activation was determined in α_{1B}AR-expressing HEK293 FRT/TO β-arrestin1/2 shRNA cells stimulated for 5 min (centre). β-arrestin1/2-dependent ERK1/2 activation was defined as the fold difference between agonist-stimulated ERK1/2 phosphorylation in the absence (total ERK1/2 signal) and presence (β-arrestin1/2-independent ERK1/2 signal) of doxycycline. A representative phospho-ERK1/2 immunoblot is shown above a graph depicting the mean ± s.e.m. of independent biological replicates ($n = 4$). EC_{50} for total ERK1/2, β-arrestin1/2-independent ERK1/2, and β-arrestin1/2-dependent ERK1/2 were 64 nM, 27 nM and 334 nM, respectively. Right, the relationship between percent maximal α_{1B}AR-induced change in FlAsH5 Δnet BRET and β-arrestin1/2-dependent ERK1/2 activation over a range of agonist concentrations. In all panels, $^*P < 0.05$, $^\#P < 0.005$, greater than nonstimulated. **b**, Relationship between GPCR-induced change in FlAsH5 Δnet BRET and arrestin-dependent ERK1/2 activation at saturating agonist concentration. The ligand-induced FlAsH5 Δnet BRET was determined in HEK293 cells transfected with the indicated GPCR and rLuc–β-arrestin2–FlAsH5 expression plasmids. The graph depicts the mean ± s.e.m. of independent biological replicates ($n = 5$).

Extended Data Table 1 | G-protein-coupling and trafficking profiles of selected GPCRs

Receptor	G protein	Arrestin binding
Angiotensin AT_{1A}	$G_{q/11}$	Class B stable binding
Parathyroid Hormone PTH_1	$G_s > G_{q/11}$	Class B stable binding
Vasopressin V_2	G_s	Class B stable binding
α_{1B} Adrenergic	$G_{q/11}$	Class A transient binding
β_2 Adrenergic	$G_s > G_i$	Class A transient binding
sphingosine 1-phosphate $S1P_1$	$G_i > G_{q/11}$	Class A transient binding
α_{2A} adrenergic	G_i	Not Detectable

Extended Data Table 2 | Primer sequences used to generate rLuc–β-arrestin2–FlAsH1–6

Primer	Sequence
RlucHindF	ATCAAGCTTGCGTTACCGGATCCATGGGTGAA
RlucApaIR	AACGGGCCCTCTAGACTAGCAGAACTGGTCA
FlAsH1F	GGATCCTGTCGATGGTTGTTGTCCTGGTTGTTGTGTGGTGCTTGTGGATC
FlAsH1R	GATCCACAAGCACCACACAACAACCAGGACAACAACCATCGACAGGATCC
FlAsH2F	GAGGACACAGGGAAGTGTTGTCCTGGTTGTTGTGCCTGTGGAGTAGAC
FlAsH2R	GTCTACTCCACAGGCACAACAACCAGGACAACACTTCCCTGTGTCCTC
FlAsH3F	GCTTATCATCAGAAAGTGTTGTCCTGGTTGTTGTGTACAGTTTGCTCCTG
FlAsH3R	CAGGAGCAAACTGTACACAACAACCAGGACAACACTTTCTGATGATAAGC
FlAsH4F	CCACGTCACCAACAATTGTTGTCCTGGTTGTTGTTCTGCCAAGACCGTCA
FlAsH4R	TGACGGTCTTGGCAGAACAACAACCAGGACAACAATTGTTGGTGACGTGG
FlAsH5F	AGCTTGAACAAGATGACCAGTGTTGTCCTGGTTGTTGTGTGTCTCCCAGTTCCACATT
FlAsH5R	AATGTGGAACTGGGAGACACACAACAACCAGGACAACACTGGTCATCTTGTTCAAGCT
FlAsH6R	ACGGGCCCTCTAGACTAACAACAACCAGGACAACAGCAGAACTGGTCATC